Supplementary Figure S1
Bianchi-Frias et al

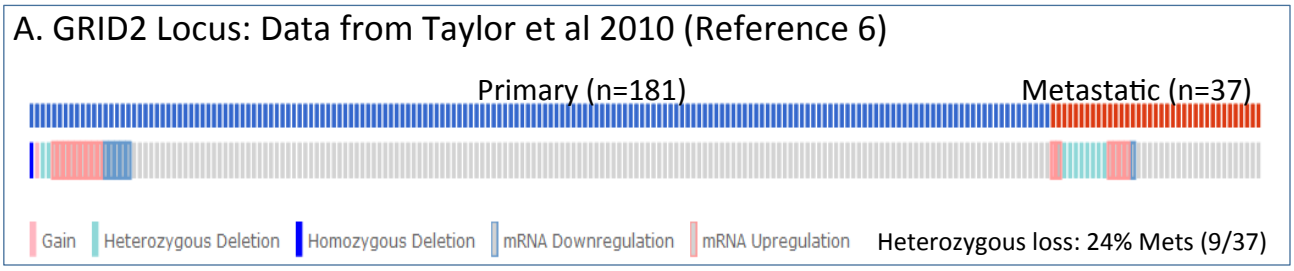


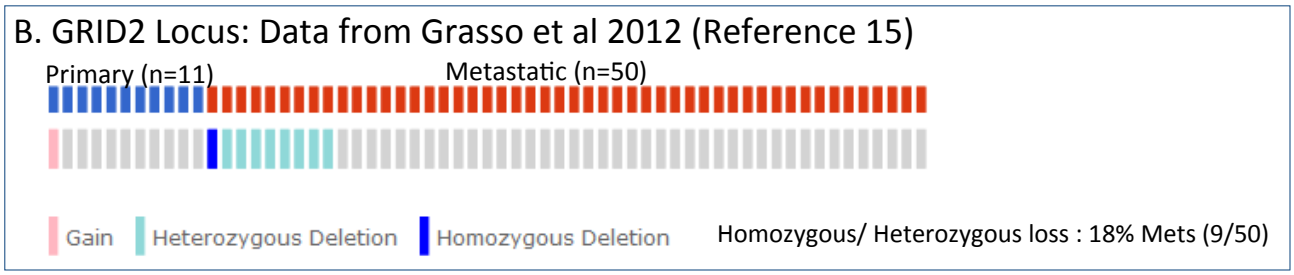


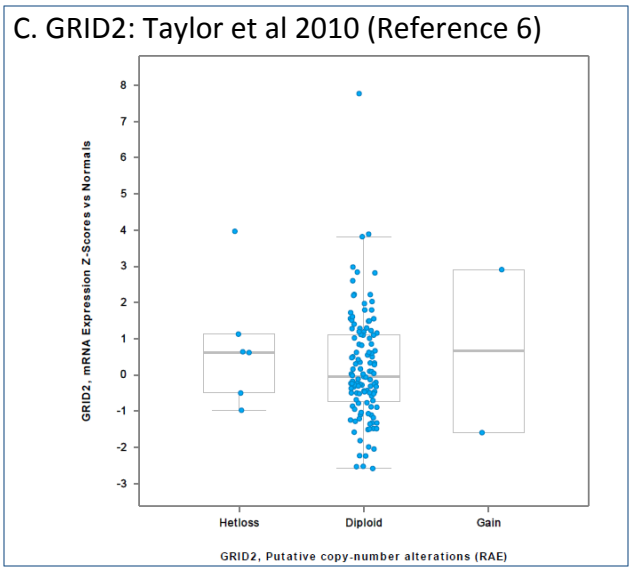


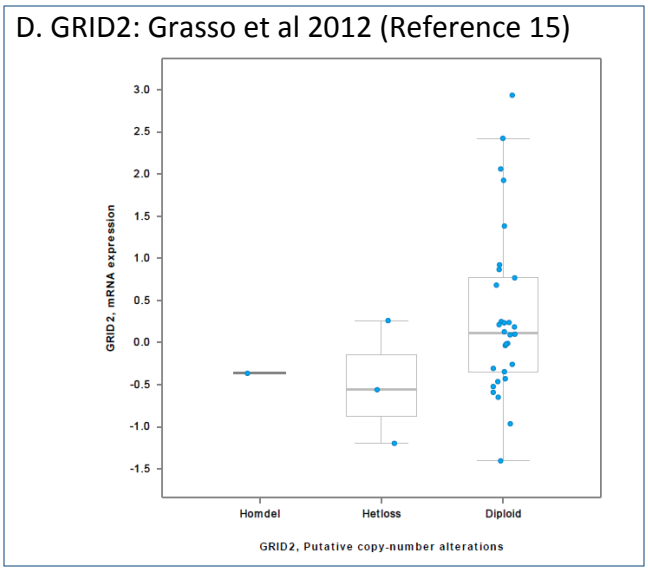

Supplementary Figure S2
Bianchi-Frias et al

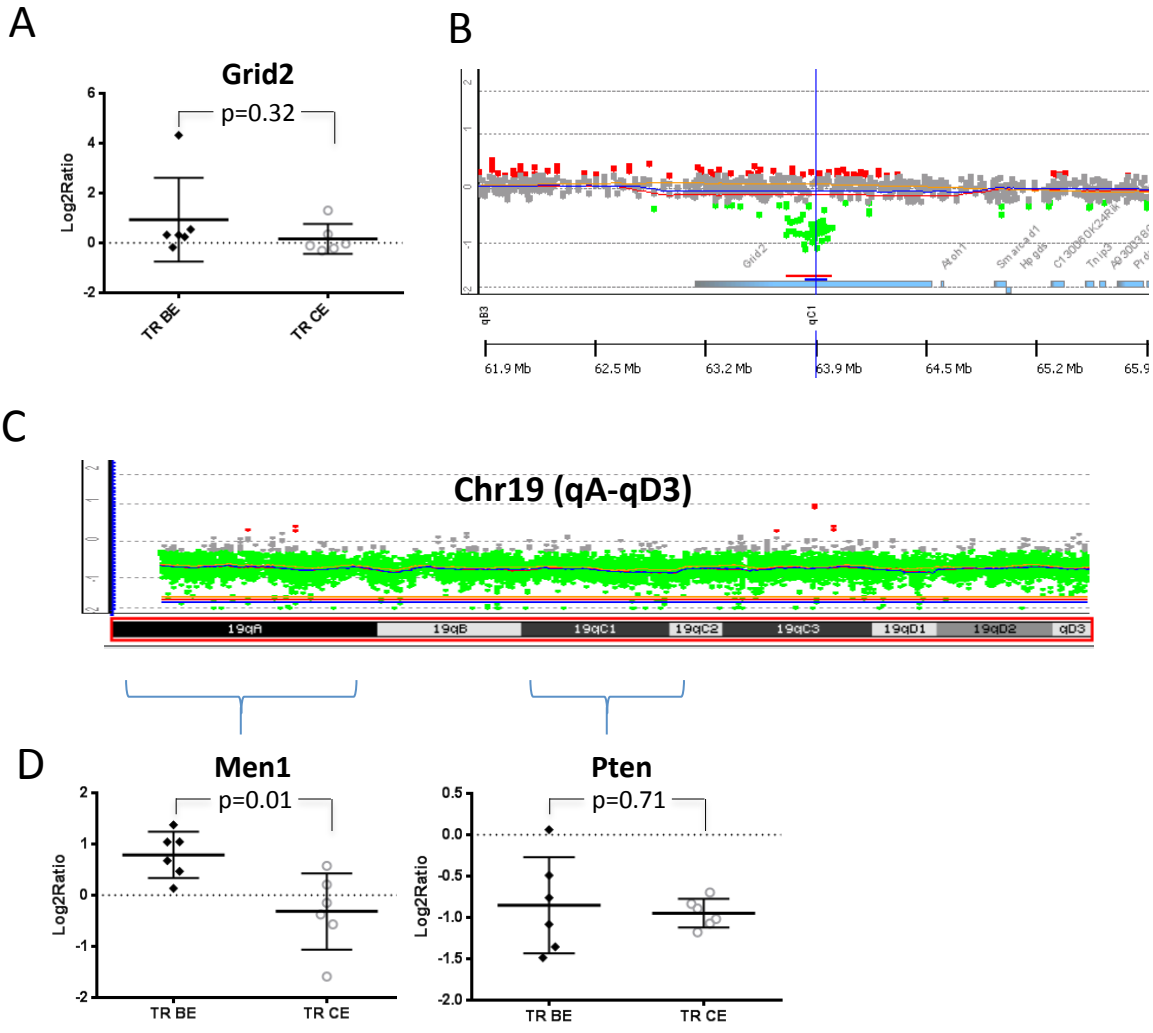

# Supplementary Figure S3

Bianchi-Frias et al

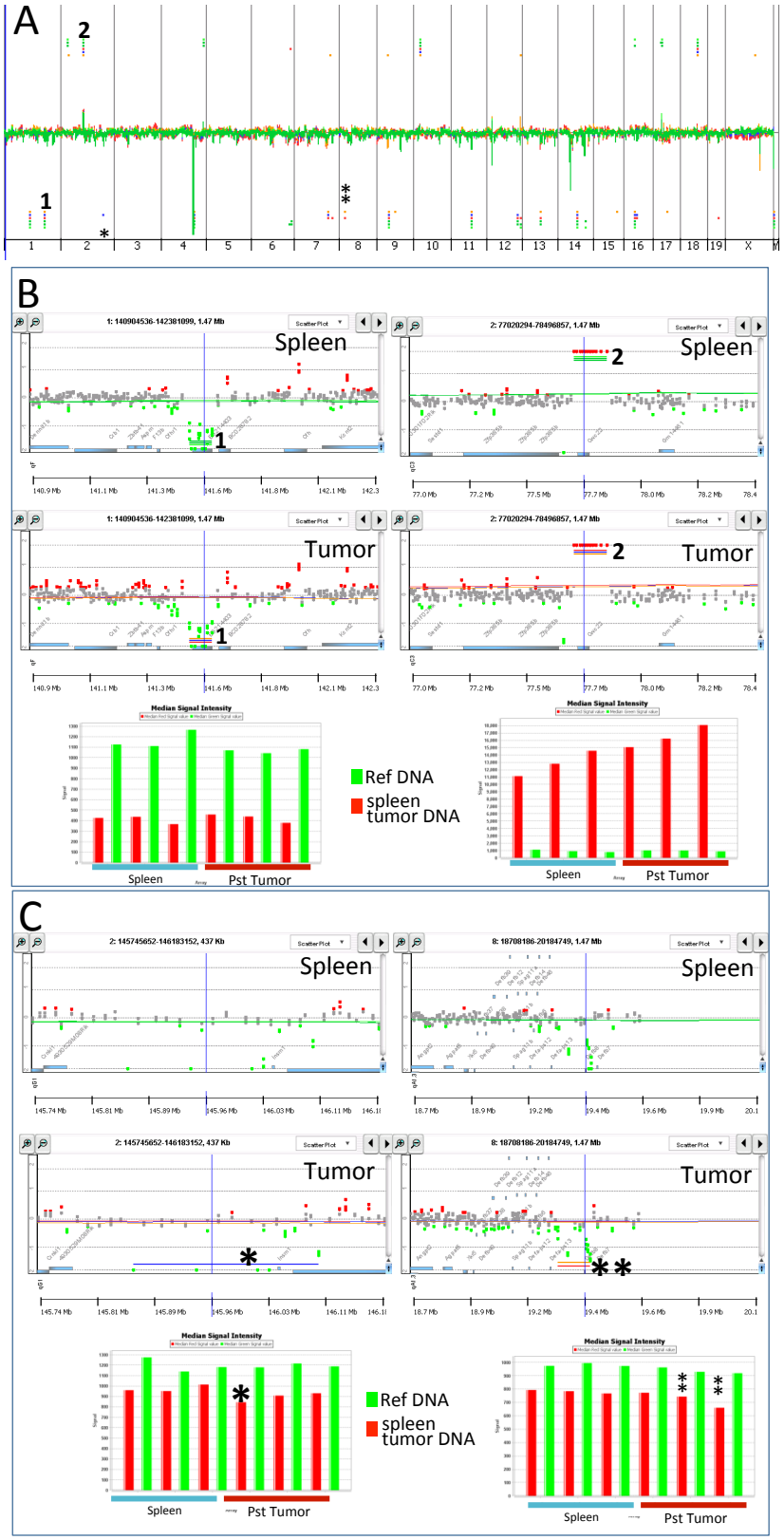

Supplementary Figure S4
Bianchi-Frias et al

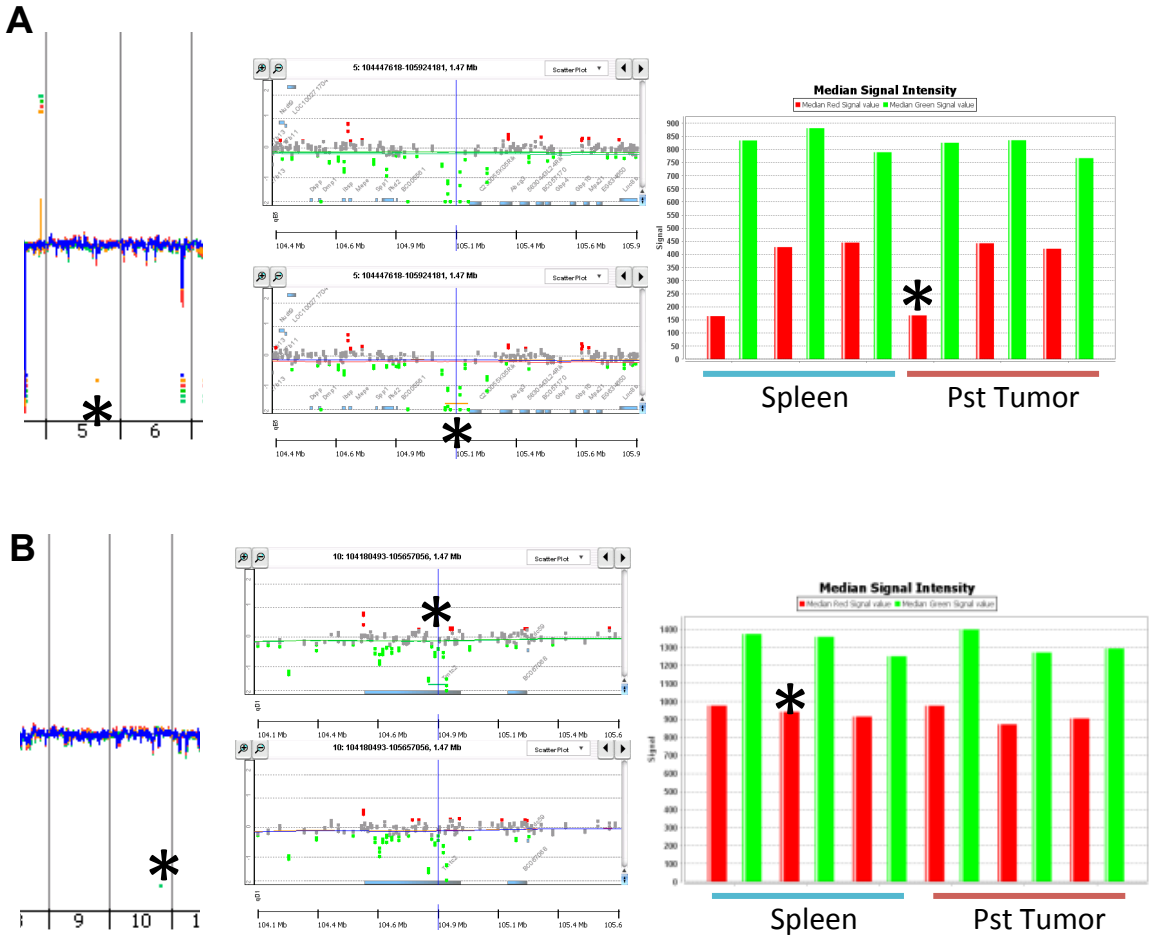

Supplementary Figure S5
Bianchi-Frias et al

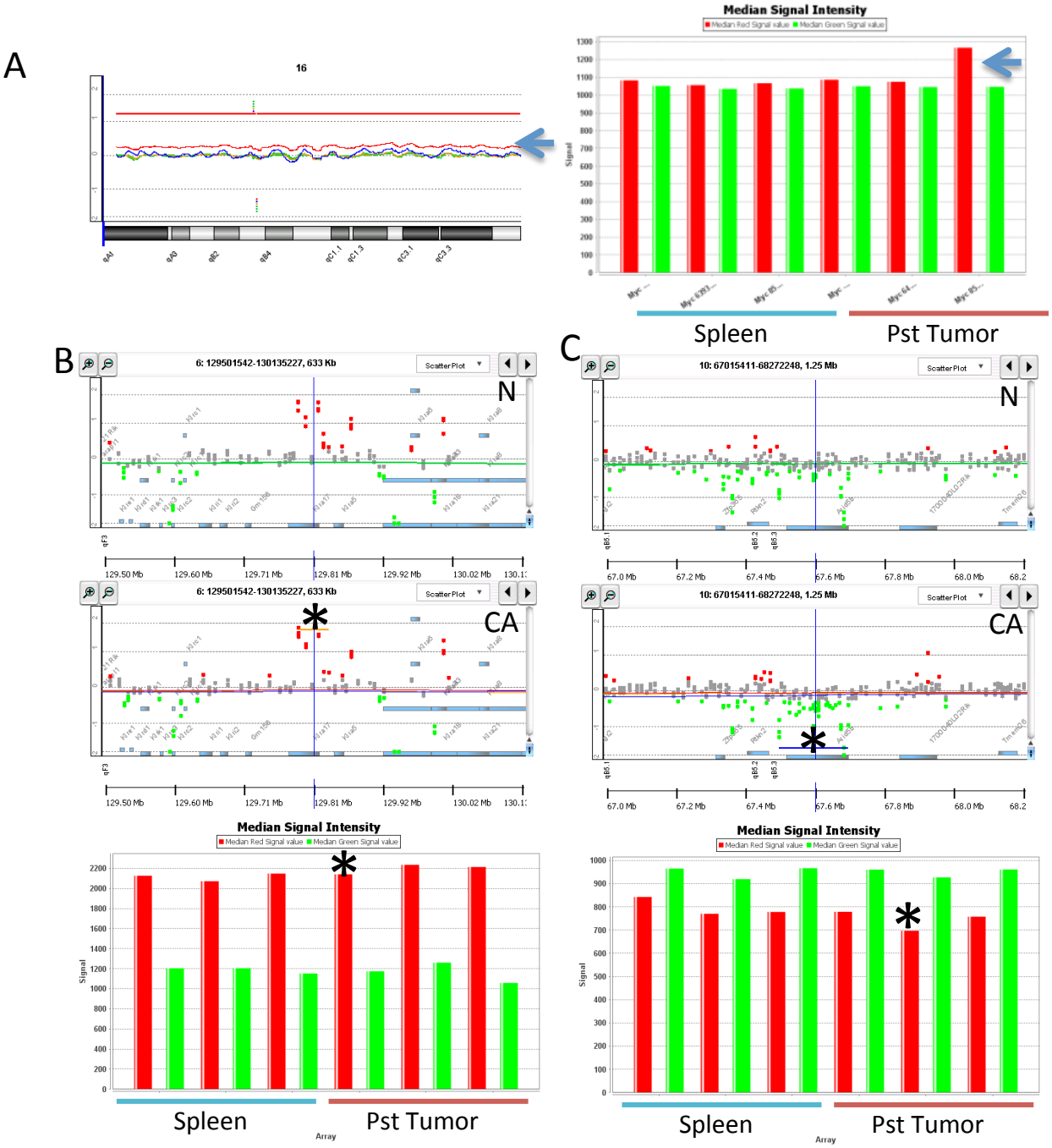

# Supplementary Figure Legends

Bianchi-Frias et al

**Figure S1.** *GRID2 genomic copy-number alterations and transcript expression in primary and metastatic prostate cancer datasets.*
Data available on the cBio Portal for Cancer Genomics were analyzed using cBio Portal tools ( http://www.cbioportal.org). We defined the genetic alterations to be shown as follows: Homdel (homozygous deletion, Hetloss: heterozygous loss, Gain, EXP < -2 mRNA under-expression is less than 2 SDs below the mean; EXP > 2 mRNA over-expression is greater than 2 SDs above the mean. **A)** Taylor et al. Cancer Cell 2010 dataset. Genomic alterations and mRNA expression of GRID2 in 181 and 37 primary and metastatic prostate cancer, respectively. **B)** Grasso et al. Nature 2012 dataset. Genomic alterations of GRID2 in 11 and 50 primary and metastatic prostate cancer, respectively. C) and D) GRID2 mRNA Expression vs. CNA in both **C)** Taylor and **D)** Grasso datasets. Of the prostate tumors assessed in these datasets, 24% and 18% of metastatic samples in Taylor and Grasso studies contained heterozygous deletion in GRID2, respectively.

**Figure S2**. *Correlation of genomic alterations and gene expression levels in TRAMP neuroendocrine carcinomas.*
**A)** Boxplots of Log2Ratios for Grid2 expression levels in benign and TRAMP neuroendocrine carcinomas (NEC) obtained by gene expression arrays. **B)** zoom-in on chromosome 6 for aberration called by the ADM-2 algorithm in the CGH array showing a SCNAs in the Grid 2 gene**. C)** Aberration called by the ADM-2 algorithm encompassing chromosome 19 showing a copy number loss of the entire chr19 in TRAMP NEC. **D)** Boxplots of Log2 Ratios for all genes located on chromosome 19 and for specific genes: Men1 and Pten, showing significant lower expression in TRAMP tumor epithelia compared to littermate benign prostate epithelium. TR BE: TRAMP Benign Epithelium, TR CE: TRAMP Cancer Epithelium . * $p<0.05$

**Figure S3**. *Analyses of genomic alterations in the LADY GEM prostate gland.*
Genomic DNA from LPB-Tag 12T-7f prostate tumors and germline spleen were hybridized against sex-matched normal mouse C57BL/6 reference DNA onto Agilent CGH arrays containing 180K probes. **A)** Whole genome view of overlaid moving averages (2 Mb window) for the log2 ratios of fluorescence between a sample/reference DNA probe (Y axis) plotted at its genomic position (X axis), **red, blue and yellow** (tumors; n=3) and **green** shades (germline n=3). Aberrations called by the ADM-2 algorithm are identified by horizontal bars. ($^{1,2}$) Representative copy number variants in common between germline and tumors (see panel B). ($^{*}$) Aberrations called by the ADM-2 algorithm in tumor samples, that by manual inspection show similar fluorescence intensities in all samples including germline and tumor (see details on panel C). **B)** Representative copy number variants in common between spleen and tumors. Zoom-in on chromosome 1 ($^{1}$ in panel A) 2 ($^{2}$ in panel A) showing overlaid data points for log2 ratios in the region, demonstrating evident copy number loss or gain, respectively, in both spleen and tumor DNA. Green: values below log2 = -0.25; Red: values above log2 = 0.25. Upper panel show spleen and lower panel shows tumors. Bar graphs showing fluorescence intensities (low, for the copy number loss) and (high, for the copy number gain) in both spleen and tumor DNA compared to reference sample. **C)** Representative aberrations called by the ADM-2 algorithm in a tumor sample that by manual inspection show similar fluorescence intensities in all samples including germline and tumor. Zoom-in on chromosome 2 and 8 ($^{*}$ in panel A) showing overlaid data points for log2 ratios in the region, demonstrating similar probe log2 ratios in both spleen and tumor DNA. Bar graphs showing similar fluorescence intensities in both spleen and tumor DNA compared to reference sample, suggesting no somatic genomic alterations in the tumor DNA compared to germline spleen DNA.

# Supplementary Figure Legends

Bianchi-Frias et al

**Figure S4.** *Genomic aberrations called in Pb-Cre;Pten $^{f/f}$ tumors by the ADM-2 algorithm in single samples that by manual inspection show similar fluorescence intensities in all samples including germline and tumor.*

Two examples **A** and **B** where manual inspection corrected a somatic CNV called by the software algorithm. For each example: Left panel, genomic view (*) copy number loss in a single Pten-null tumor sample. Middle panel: zoom-in on chromosome 5, demonstrating similar log2 ratios for probes in that region for both spleen and tumor DNA. Right panel, bar graphs showing similar fluorescence intensities in both spleen and tumor DNA compared to reference sample, suggesting no somatic genomic alterations in the tumor DNA compared to germline spleen DNA.

**Figure S5**. *Manual inspection of genomic aberrations in the Hi-Myc GEM model*.

**A,** Whole chromosome 16 view of overlaid moving averages (2 Mb window) for the log2 ratios of fluorescence between a sample (germline and c-Myc tumor DNA) and reference (sex-matched normal mouse C57BL/6) DNA probe. **Red, blue and yellow** (tumors; n=3) and **green** shades (germline n=3), showing gain of whole chromosome 16 on one tumor sample (arrow). Bar graph showing high intensity levels for the tumor with a gain on chr 16 (arrow) compared to the other 2 c-myc tumor samples or spleen DNA. **B** and **C,** aberrations called by the ADM-2 algorithm in single c-Myc tumor samples that by manual inspection show similar fluorescence intensities in all samples including germline and tumor. (*) single samples called for the aberration. Note in the bar graph similar intensity levels (red bars) for all spleen and tumor samples, demonstrating that the aberration is not unique to tumor samples.